Understanding Properties of the Proton from Holographic Models

Ayrton da Cruz Pereira do Nascimento

INSTITUTO DE FÍSICA, UNIVERSIDADE FEDERAL DO RIO DE JANEIRO

in collaboration with Henrique Boschi (IF-UFRJ)

6th WONPAQCD, UTFSM Valparaiso, Chile

December 2nd, 2025

1. Proton's Gravitational Form Factors and Mechanical Properties

2. Proton's Structure Function

1: arXiv:2511.20715

2: work in progress

Physical Problem: Proton's Mechanical Properties

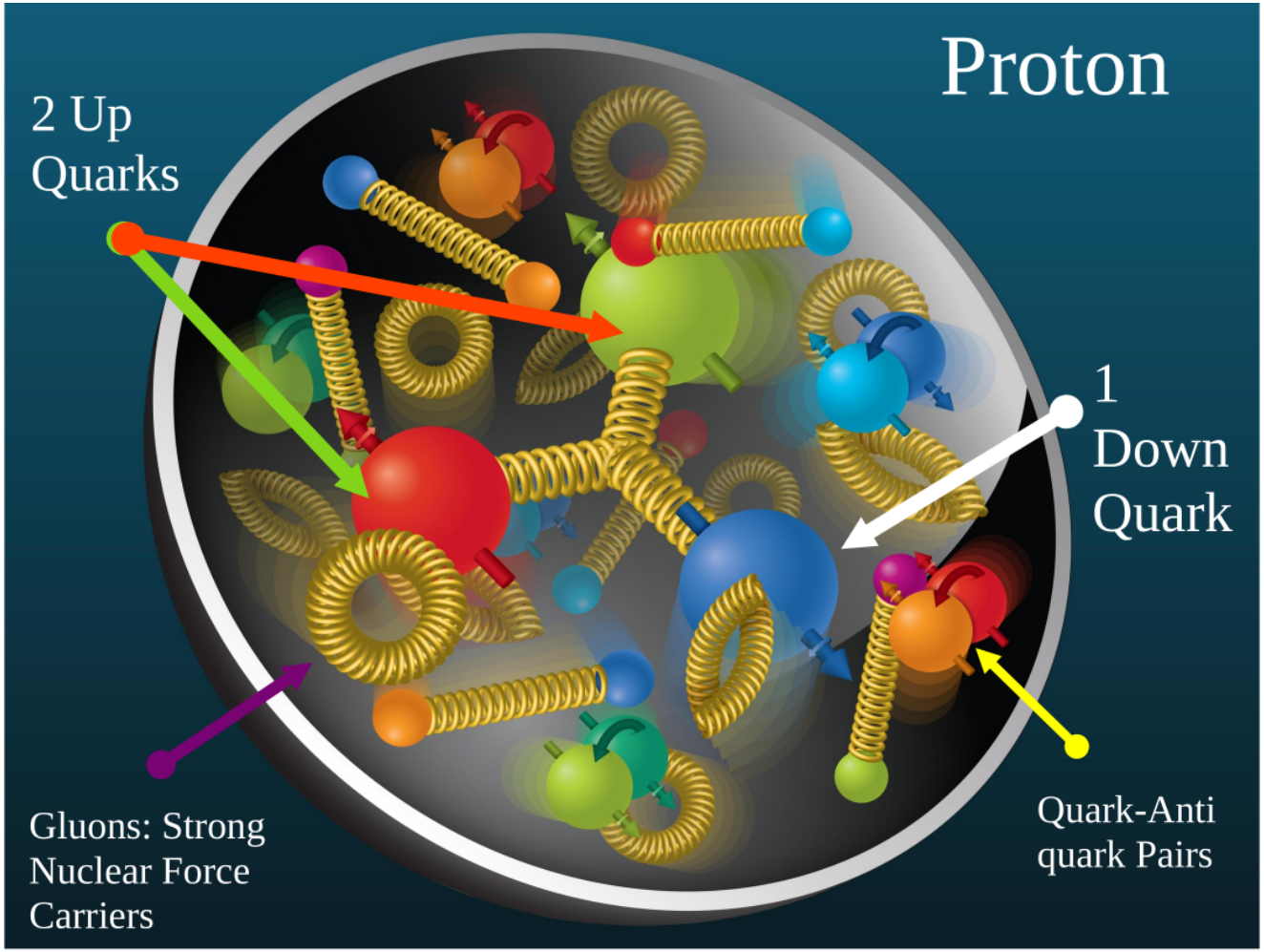

Adapted from `https://www.bnl.gov/eic/`

Physical Problem: Proton's Mechanical Properties

We look for mechanical properties by stuying the proton's energy momentum tensor matrix elements [Polyakov and Schweitzer, 2018]

$$\langle p_2|\, T^{\mu\nu}(0)\, |p_1\rangle = \bar{u}(p_2)\left[A(q)\,\gamma^{(\mu}p^{\nu)} + B(q)\,\frac{i\,p^{(\mu}\sigma^{\nu)\alpha}q_\alpha}{2\,m_p} + C(q)\,\frac{q^\mu q^\nu - \eta^{\mu\nu}q^2}{m_p}\right]u(p_1), \tag{1}$$

$q = p_2 - p_1$. A, B and C are gravitational form factors (GFFs) related, respectively, to the momentum distribution, spin and angular momentum distribution, and internal forces distributions such as pressure and shear.

Holographic Gauge/Gravity Duality

Juan Maldacena [Maldacena, 1998]: Equivalence Between

5D Classical Gravity in anti-de Sitter Geometry $\Longleftrightarrow$ $3+1$D Strongly Coupled QFT in Minkowski Spacetime.

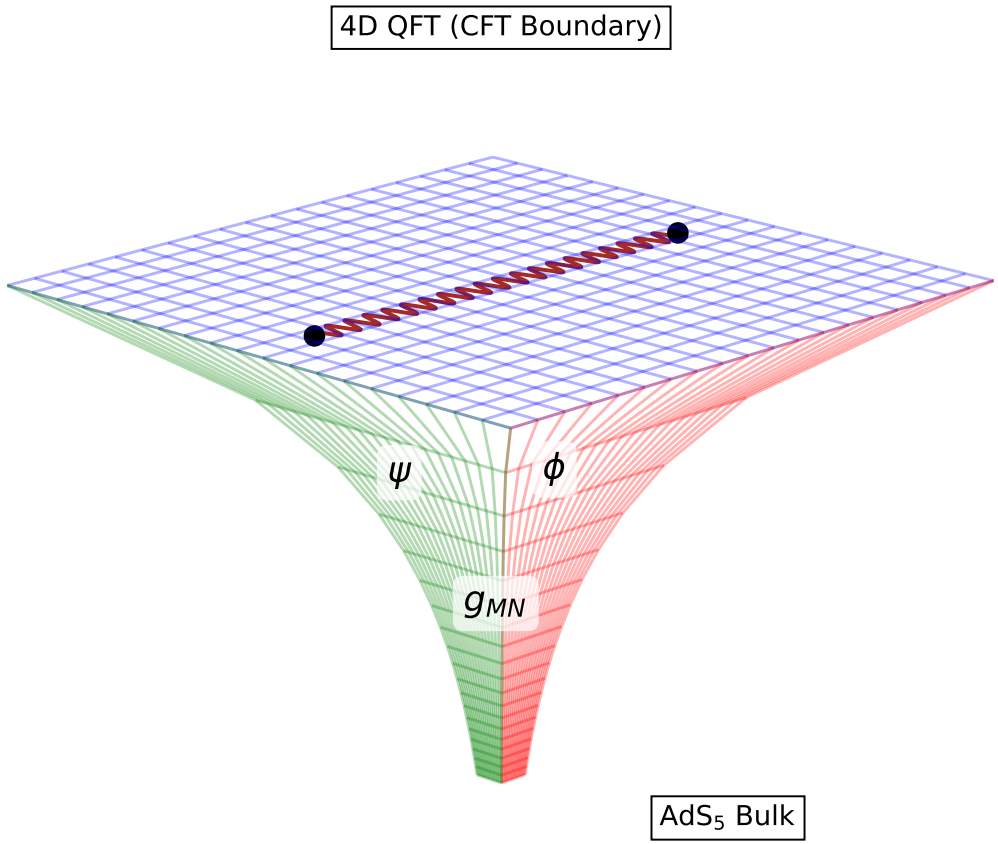

Deformed AdS Model

Deformed anti-de Sitter (AdS) Geometry

$$S = \int d^5x \sqrt{-g}\, \mathcal{L}. \tag{2}$$

Probe fields are defined in a bulk five-dimensional spacetime with metric

$$ds^2 = g_{MN}\, dx^M dx^N = e^{\mathcal{A}(z)}(dz^2 + \eta_{\mu\nu}\, dx^\mu dx^\nu), \tag{3}$$

$$\mathcal{A}(z) = -\log(z/R) + \phi(z), \tag{4}$$

$\phi(z) = \frac{1}{2}\kappa\, z^2$, $\kappa[\text{mass}^2]$, gives a confining $q\,\bar{q}$ potential [Andreev and Zakharov, 2006]. Conformal Theory on AdS at $z \to 0$.

Holographic Dictionary: ϕ is dual to $\text{Tr}\{F^2\}$ (gluon condensate).

Probe Fields

To compute GFFs in holography, we need two probe fields: the metric (graviton) and a fermionic field Ψ (representing the proton)

Fermions

$$S_F = \int dz\, d^4x\, \sqrt{-g}\, \bar{\Psi}(\not{D} - m_5)\Psi, \tag{5}$$

where m_5 is the fermion mass in the deformed background. From this one can obtain

$$[-\partial_z^2 + V_{L/R}(z)]\, \psi^n_{L/R}(z) = M_n^2\, \psi^n_{L/R}(z), \tag{6}$$

$$V_{L/R}(z) = m_5^2\, e^{2\,\mathcal{A}(z)} \mp e^{\mathcal{A}(z)}\, m_5\, \mathcal{A}'(z). \tag{7}$$

Probe Fields

To compute GFFs in holography, we need two probe fields: the metric (graviton) and a fermionic field Ψ (representing the proton)

The Metric g_{MN}

$$S_g = \frac{1}{16\pi\, G_N} \int dz\, d^4x \sqrt{-g}\, (R - 2\Lambda), \tag{8}$$

with $R = g_{MN} R^{MN}$ the Ricci scalar.

Energy Momentum Tensor and Graviton

The EMT is taken by the expression

$$T^{\mu\nu}(x) = \frac{2}{\sqrt{-g}} \frac{\delta\, S_{\text{grav}}}{\delta\, g^{\mu\nu}(x)}. \tag{9}$$

In the bulk geometry, it sources a fluctuation in the metric

$$g_{MN}(z) \to \eta_{MN}(z) + h_{MN}(z). \tag{10}$$

Form factors come out of the coupling between h_{MN} and the fermionic solutions in (9), where we choose $S_{\text{grav}} = S_F$. To match the EMT tensor structure, we decompose h_{mn} as

$$h_{MN}(q,z) = \underbrace{\epsilon^{TT}_{MN}\, h(q,z)}_{\text{transverse-traceless}} + \underbrace{q_M\, q_N\, H(q,z)}_{\text{tracefull}}. \tag{11}$$

Fit and Comparison to Lattice QCD Results

$$A(q^2) = \frac{1}{2}\int dz\, e^{-5\,\mathcal{A}(z)}(\psi_L^2 + \psi_R^2)\, h(q^2, z), \tag{12}$$

$$C(q^2) = \frac{1}{2}\int dz\, e^{-5\,\mathcal{A}(z)}\, H(q, z)\, \psi_L\, \psi_R. \tag{13}$$

We will also need the following definition $D(q^2) \equiv 4\, C(q^2)$.

- Normalization by $A(0)$, $D(0)$ from lattice QCD [Hackett et al., 2024]
- χ^2 minimization
- Best fit $A(q^2)_{\text{norm}}$, $D(q^2)_{\text{norm}}$

Fit and Comparison to Lattice QCD Results

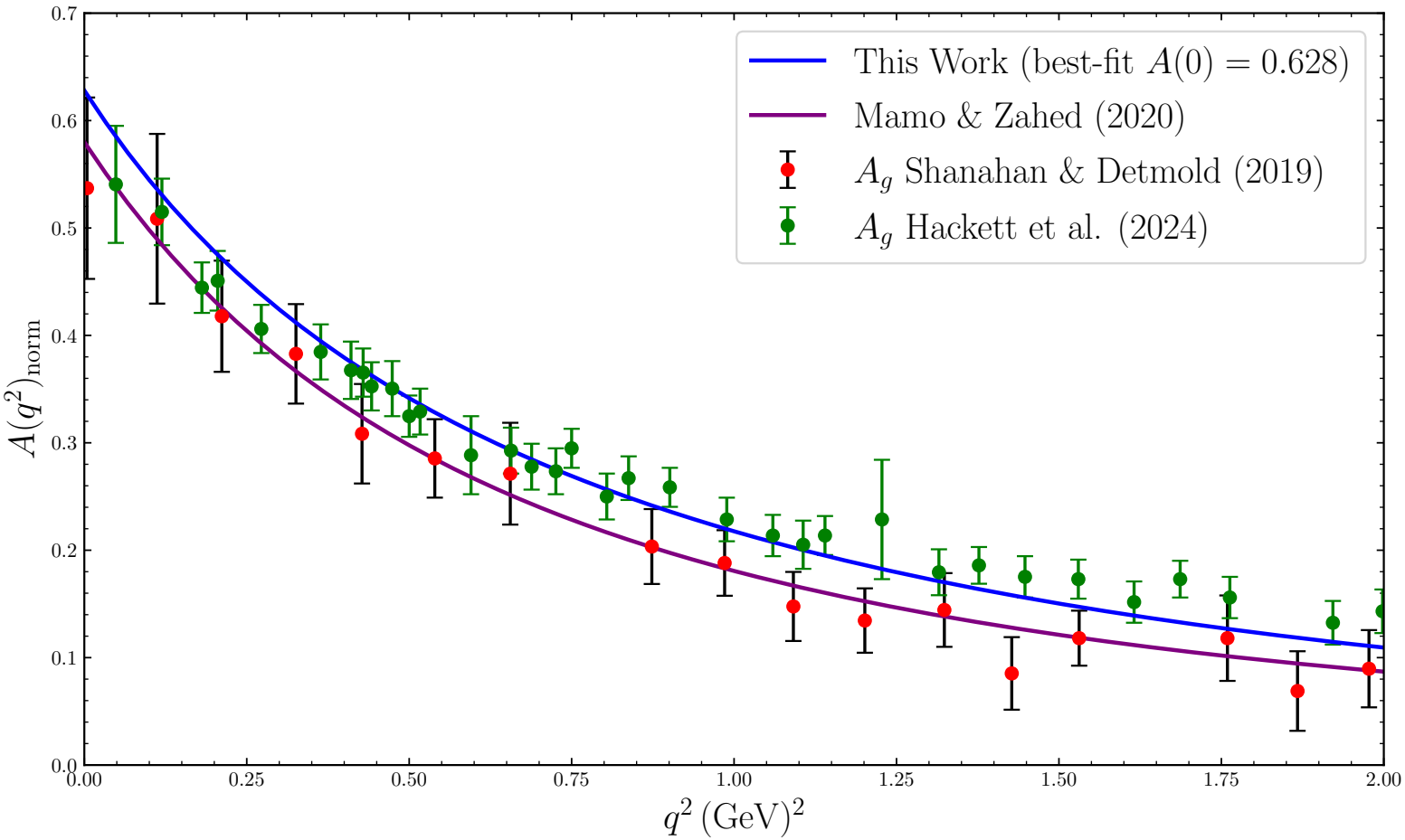

$A(q^2)$ fit by normalizing our result by $A(0) = 0.628$. Also compared with data from [Hackett et al., 2024].

Fit and Comparison to Lattice QCD Results

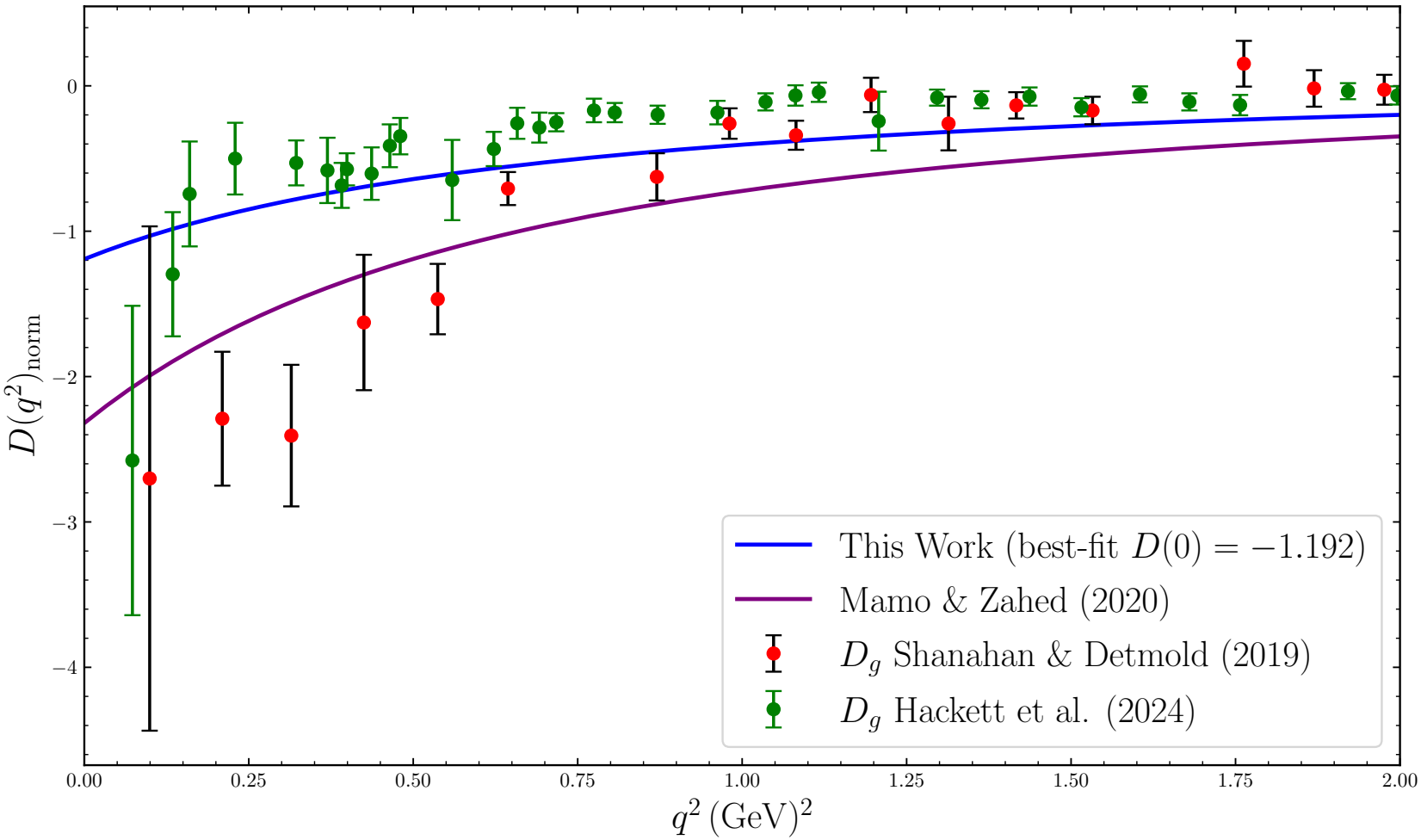

$D(q^2)$ fit by normalizing our result by $D(0) = -1.192$. Also compared with data from [Hackett et al., 2024].

Pressure and Shear Distributions

By taking the following Fourier transformation

$$\tilde{D}(r) = \int \frac{d^3q}{2\,m_p\,(2\pi)^3} e^{-i\,q\cdot r} D(q^2), \tag{14}$$

we can compute pressure and shear distributions inside the proton [Polyakov and Schweitzer, 2018]

$$p(r) = \frac{1}{6\,m}\frac{1}{r^2}\frac{d}{d\,r}\left(r^2\frac{d}{d\,r}\tilde{D}(r)\right), \tag{15}$$

$$s(r) = -\frac{r}{4\,m}\frac{d}{d\,r}\left(\frac{1}{r}\frac{d}{d\,r}\tilde{D}(r)\right). \tag{16}$$

$m = 0.938\,\text{GeV}$ is the proton mass.

Pressure and Shear Distributions

For numerical convenience, we choose a dipole approximation to our numerical $D(q^2)$ result. A very good approximation is found with

$$D(q^2) = \frac{D_0}{\left(1 + \frac{q^2}{\Lambda^2}\right)^2}, \tag{17}$$

A very good approximation is found with $D_0 = -1.196$ and $\Lambda = 1.165\,\text{GeV}$.

Pressure and Shear Distributions

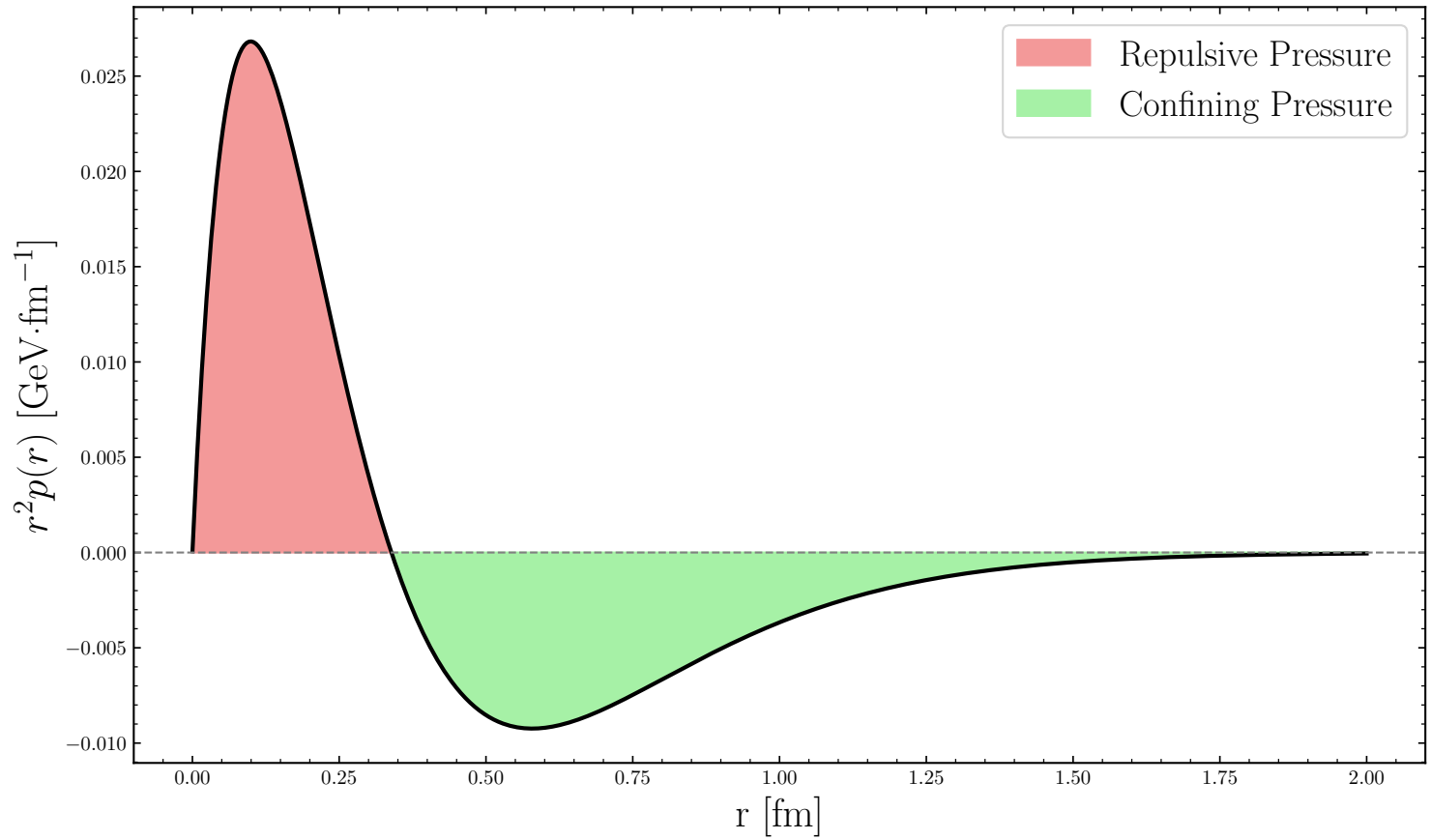

Pressure distribution inside the proton from the dipole approximation. This integrates to 2.31×10^{-6} *GeV.*

$$\text{Stability condition: } \int_0^\infty r^2\, p(r)\, dr = 0. \tag{18}$$

Pressure and Shear Distributions

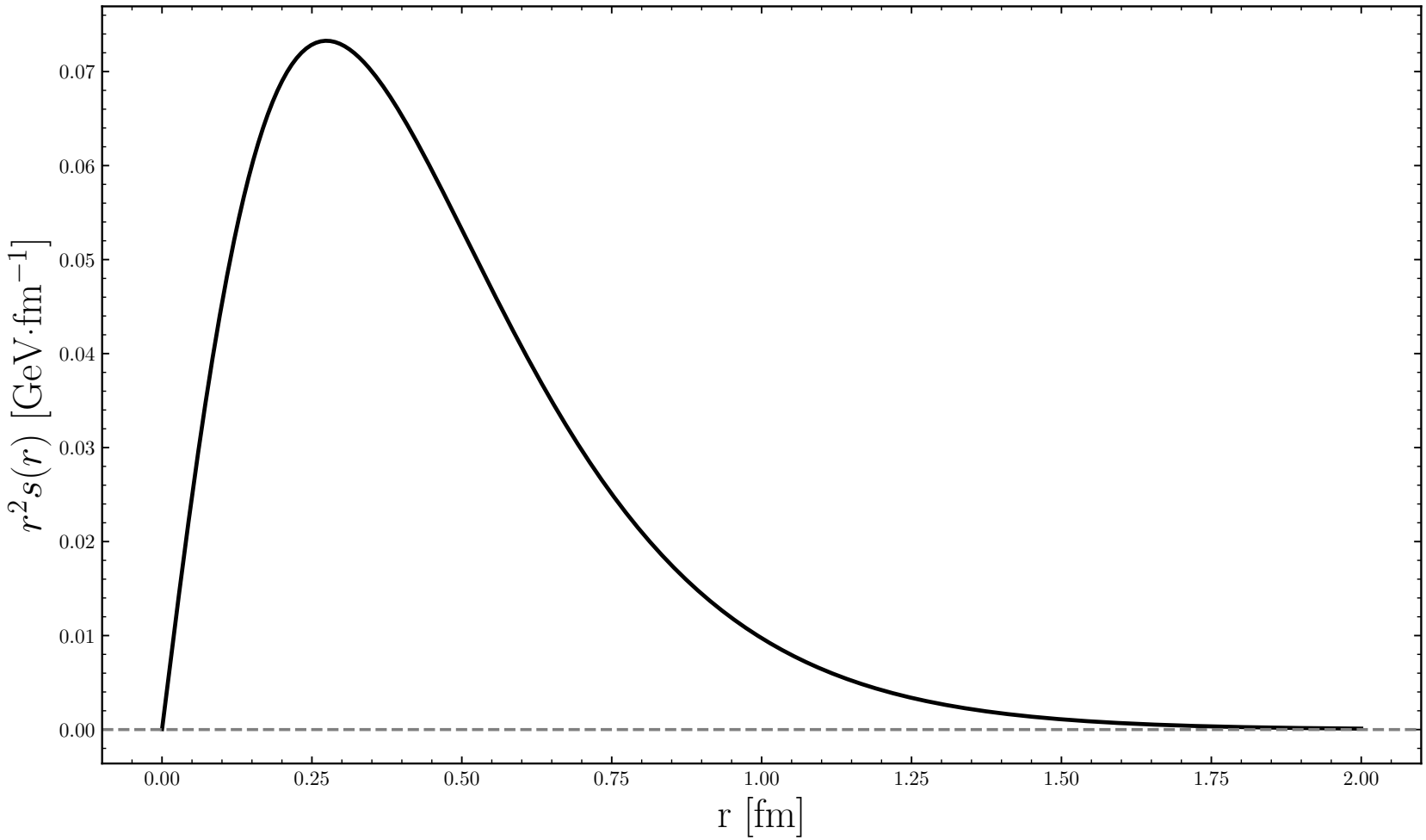

Shear distribution inside the proton from the dipole approximation.

Energy Density

The energy distribution in the system is obtained by

$$\epsilon(r) = m \left[A(q^2) + \frac{q^2 (D(q^2) + A(q^2) - 2\, B(q^2))}{4\, m^2} \right]_{\mathrm{FT}} . \tag{19}$$

We use a dipole approximation to our numerical $A(q^2)_{\mathrm{norm}}$

$$A(q^2) = \frac{A_0}{\left(1 + \frac{q^2}{\lambda^2}\right)}, \tag{20}$$

with A_0 and λ free parameters. The best approximation is found with $A_0 = 0.627$ and $\lambda = 1.186\,\mathrm{GeV}$.

Energy Density

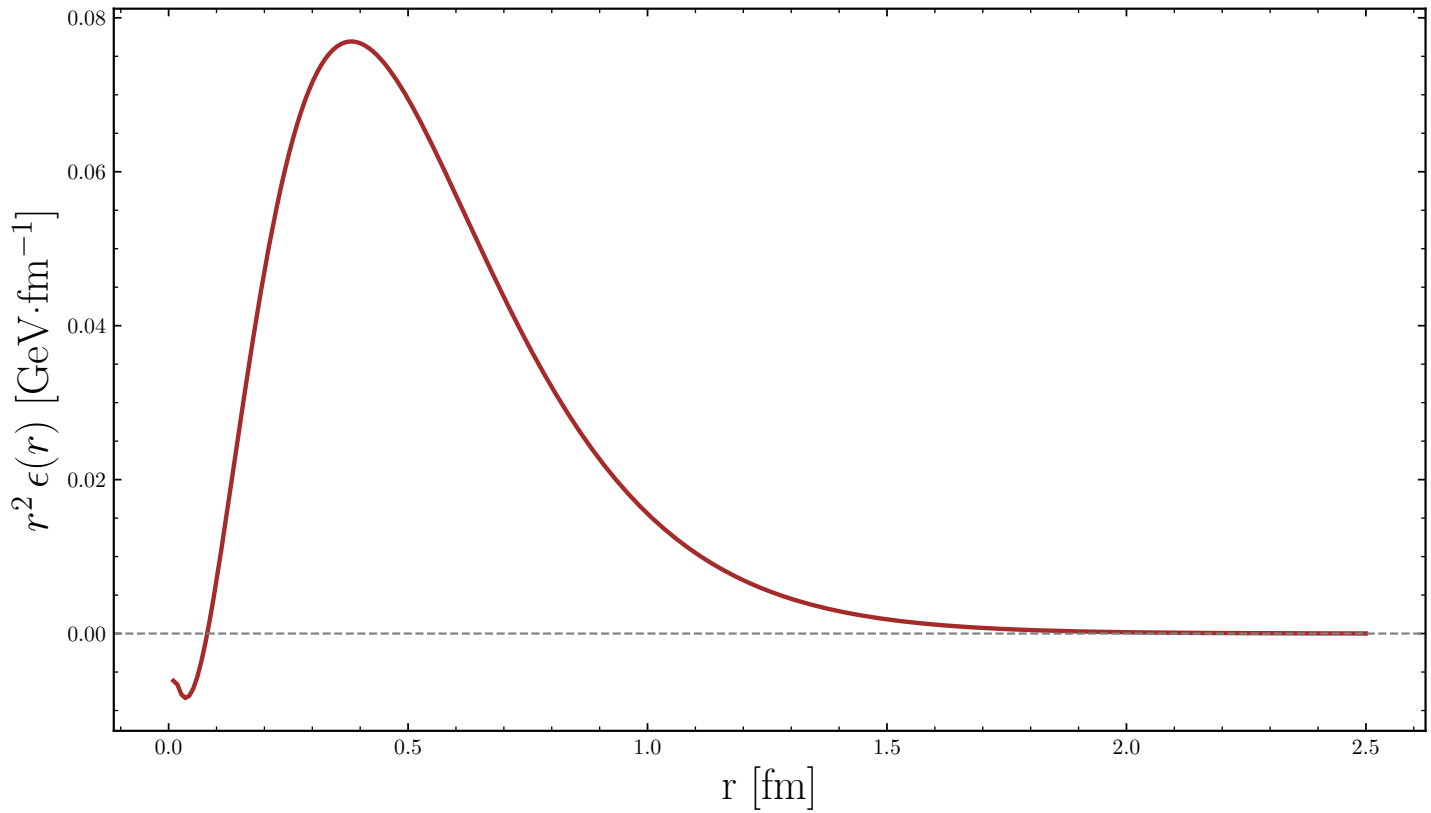

Energy distribution inside the proton from the dipole approximation.

Energy Density

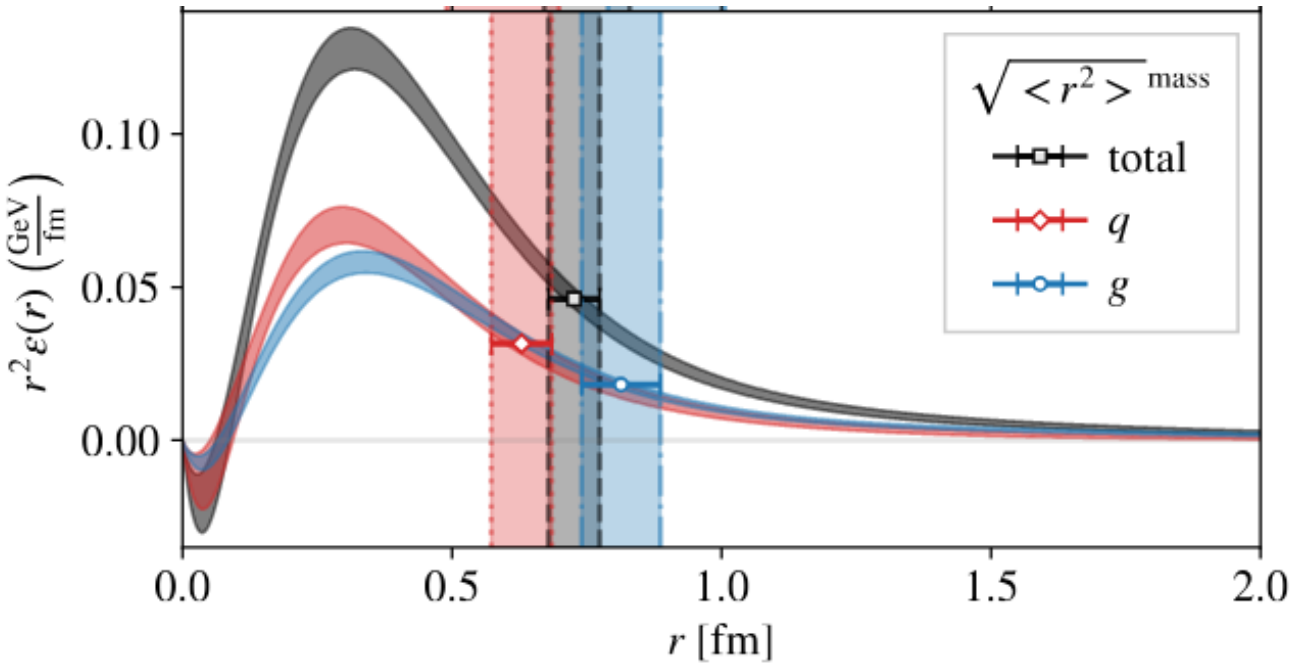

Energy distributions inside the proton from lattice QCD approach of [Hackett et al., 2024].

Mechanical Radii

We can also compute the following mechanical radii associated, respectively, with the momentum distribution and internal forces distributions [Polyakov and Schweitzer, 2018]

$$\langle r_g^2 \rangle = -6 \left(\frac{d \ln A(q^2)}{d\, q^2} \right) \Bigg|_{q=0} = (0.59\,\mathrm{fm})^2, \tag{21}$$

$$\langle\, r^2_{\mathrm{mech}} \rangle = \frac{6}{\Lambda^2} = (0.42\,\mathrm{fm})^2. \tag{22}$$

$\langle\, r^2_{\mathrm{LQCDmech}} \rangle = (0.51\,\mathrm{fm})^2$ [Shanahan and Detmold, 2019] and $\langle\, r^2_{\mathrm{charge}} \rangle = (0.84\,\mathrm{fm})^2$ [Navas et al., 2024].

Physical Problem: Deep Inelastic Scattering

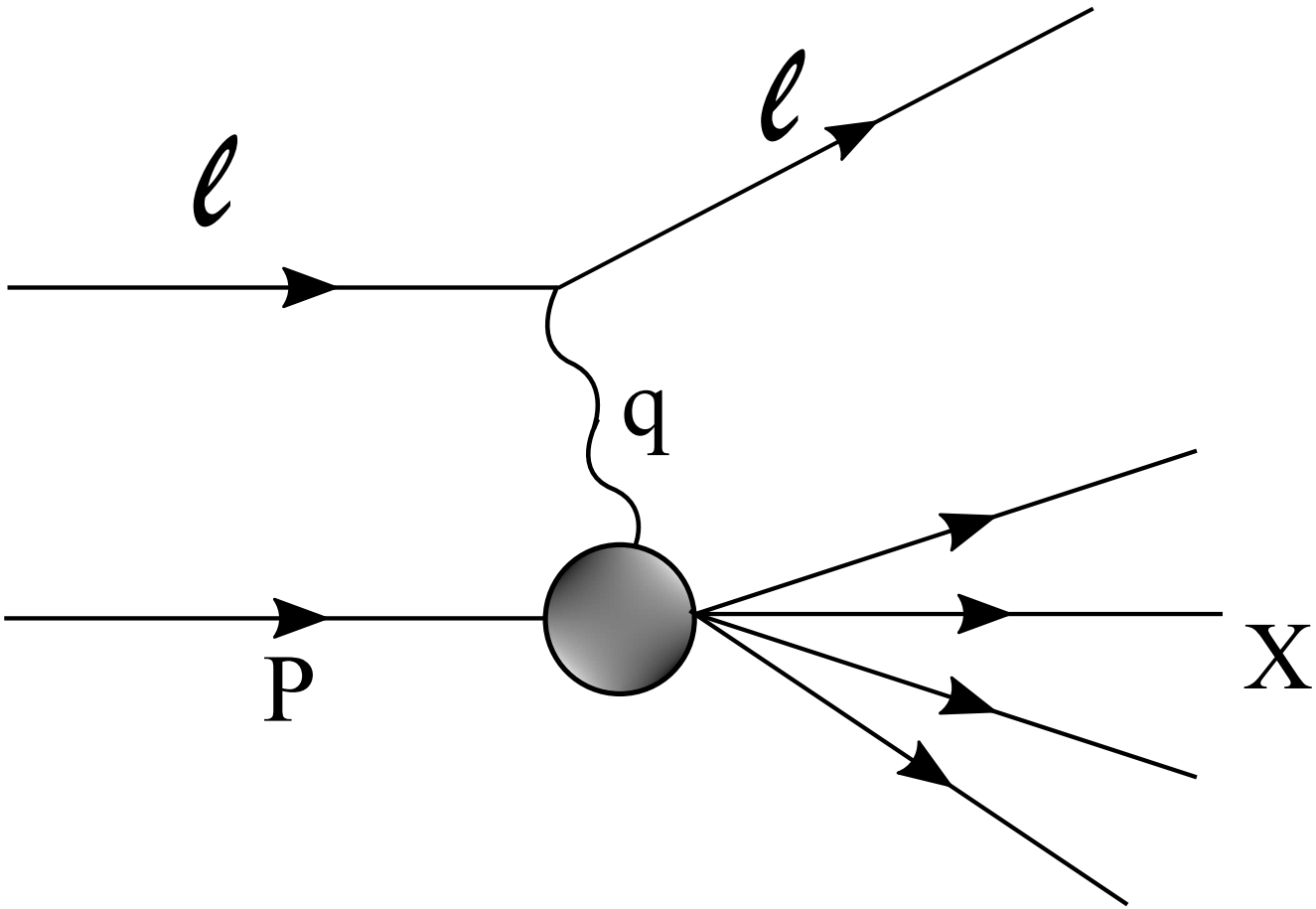

Physical Problem: Deep Inelastic Scattering

We look for structure functions by studying the hadronic tensor

$$W^{\mu\nu} = \frac{1}{4\,\pi} \sum_{s} \int d^4y \; e^{iq.y} \langle P, s| \left[J^{\mu}(y) \, , J^{\nu}(0) \right] |P, s\rangle, \tag{23}$$

which, for unpolarized targets, can be cast as

$$W^{\mu\nu} = F_1(x,q) \left(\eta^{\mu\nu} - \frac{q^{\mu} q^{\nu}}{q^2} \right) + \frac{2x}{q^2} F_2(x,q) \left(P^{\mu} + \frac{q^{\mu}}{2x} \right) \left(P^{\nu} + \frac{q^{\nu}}{2x} \right), \tag{24}$$

where $x = -q^2/(2P \cdot q)$ is the momentum fraction carried by the parton (that is, the parameter Bjorken x), and $F_{1,2}(x,q)$ are the unpolarized DIS structure functions, with $0 \leq x \leq 1$ and $q^2 > 0$.

Holographic Prescription

The hadronic tensor can be computed by evaluating the matrix element [Polchinski and Strassler, 2003]

$$\langle X\,|J^{\nu}(0)|\,P,s\rangle = S_{\text{int}} = \int dz\,d^4y\,\sqrt{-g}\,e^{F(z)}\mathcal{A}^m\,\bar{\Psi}_X\,\Gamma_m\,\Psi_i, \qquad (25)$$

where $F(z)$ is an effective scale dependent coupling between the photon field $\mathcal{A}^m$ and the initial and final fermionic states Ψ_i and Ψ_X.

Holographic Einstein-Dilaton model

We start with a general Einstein-Dilaton action (with at most two derivatives) in the Einstein frame to describe the bulk

$$S = \frac{1}{8\pi G_5} \int d^5x \sqrt{-g} \left[\mathcal{R} - \frac{1}{2} \left(\partial_\mu \phi \right) \left(\partial^\mu \phi \right) - V(\phi) \right], \tag{26}$$

with G_5 being Newton's constant in five dimensions. We consider a general background with line element [Gubser and Nellore, 2008]

$$ds^2 = g_{mn} dx^m dx^n = e^{2A(\phi)} \eta_{\mu\nu} dx^\mu dx^\nu + e^{2B(\phi)} d\phi^2. \tag{27}$$

Holographic Einstein-Dilaton model

The equations of motion are

$$A'' - A'B' + \frac{1}{6} = 0 \tag{28}$$

$$24(A')^2 - 1 + 2e^{2B}V = 0 \tag{29}$$

$$4A' - B' - e^{2B}V' = 0. \tag{30}$$

Dilaton Potential

Inspired by [Finazzo and Noronha, 2014], we choose their $V(\phi)$ as

$$V(\phi) = -\frac{12}{R^2}(1 + a\phi^2)^{1/4}\cosh(\beta\phi) + \frac{b_2\phi^2 + b_4\phi^4 + b_6\phi^6}{R^2}. \tag{31}$$

a	β	b_2	b_4	b_6
1	$\sqrt{2/3}$	5.5	0.3957	0.0135

Tabela 1: Parameters of the potential $V(\phi)$ (using units where the AdS radius $R = 1$).

Holographic Einstein-Dilaton model

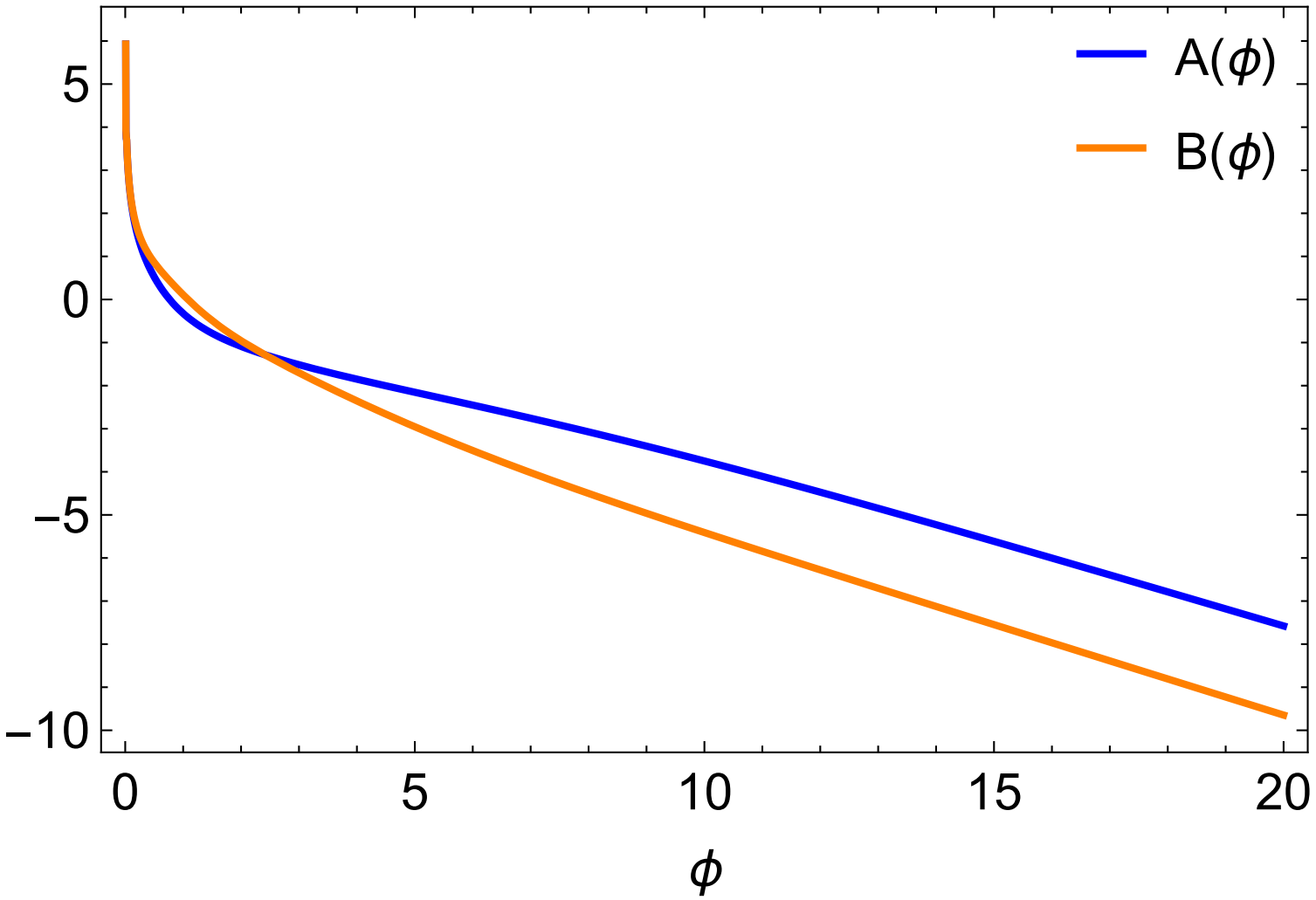

Numerical $A(\phi)$ and $B(\phi)$ functions. They determine the geometry of the curved spacetime.

Probe Fields

In this case we have a photon and a fermionic field as probes of the DIS process.

$$S_{\text{photon}} = -\int d^5x\sqrt{-g}F^{mn}F_{mn}, \tag{31}$$

$$S_{\text{fermion}} = \underbrace{\int d^5x\sqrt{-g}\ \bar{\Psi}(\not{D} - \tilde{m}_5)\Psi}_{\text{Caveat: not confining!}}, \tag{32}$$

Probe Fields

In this case we have a photon and a fermionic field as probes of the DIS process.

$$S_{\text{photon}} = -\int d^5x\sqrt{-g}F^{mn}F_{mn}, \tag{31}$$

$$S_{\text{fermion}} = \underbrace{\int d^5x\sqrt{-g}\;\bar{\Psi}(\not{D} - \tilde{m}_5)\Psi}_{\text{Caveat: not confining!}}, \tag{32}$$

We use $A \approx B + \text{constant}$ to get

$$-\psi^{n\,\prime\prime}_{R/L}(\phi) + V_{L/R}(\phi)\psi^n_{R/L}(\phi) = \left(\frac{M_n}{2}\right)^2 \psi^n_{R/L}(\phi), \tag{33}$$

with the right and left potentials given by

$$V_{R/L}(\phi) = \tilde{m}_5 e^B \left(\tilde{m}_5 e^B \pm B'\right). \tag{34}$$

For the potentials to confine, we set $\tilde{m}_5 e^B = m_5\, B$.

Interaction Action

We can evaluate $S_{\rm int}$ with the solutions of the probe fields. Choosing $F(z=\phi)=kB(\phi)$, one can get

$$\begin{aligned} S_{\rm int} &= \int d\phi\, d^4y\, \sqrt{-g}\, e^{kB(\phi)}\mathcal{A}^m\, \bar{\Psi}_X\, \Gamma_m\, \Psi_i \\ &= \pi^4\, \delta^4(P_X - P - q)\; \eta^\mu \left[\bar{u}_{s_X}\, \gamma_\mu\, \hat{P}_R\, u_{s_i}\, \mathcal{I}_L + \bar{u}_{s_X}\, \gamma_\mu\, \hat{P}_L\, u_{s_i} \mathcal{I}_R\right], \end{aligned} \tag{35}$$

with

$$\mathcal{I}_{R/L} = \int d\phi\, e^{\tilde{k}B} f(\phi, q)\, \psi^X_{R/L}(\phi, P_X)\, \psi^i_{R/L}(\phi, P)\,. \tag{36}$$

$f(\phi, q)$ is a function related to the photon solution.

Structure Function F_2

All these steps allows us to evaluate the matrix element $\langle X\,|J^{\nu}(0)|\,P,s\rangle = S_{\text{int}}$ present in the hadronic tensor, and then evaluate the latter to extract structure functions, such as F_2

$$F_2(q^2,x) = \frac{\left(\pi^4\, g_{\text{eff}}\right)^2}{2}\frac{q^2}{x}\left(\mathcal{I}_L^2+\mathcal{I}_R^2\right)\frac{1}{M_X^2}. \tag{37}$$

Structure Function F_2

x	g_{eff}	$\tilde{k}$
0.55	0.715	1.5
0.65	0.317	1.5
0.75	0.213	0.5
0.85	0.126	1.3

Tabela 1: *The values of the free parameters g_{eff} and $\tilde{k}$ used to adjust the lines calculated using Eq. (37) to compare with the available experimental data points for the proton structure function F_2.*

Structure Function F_2

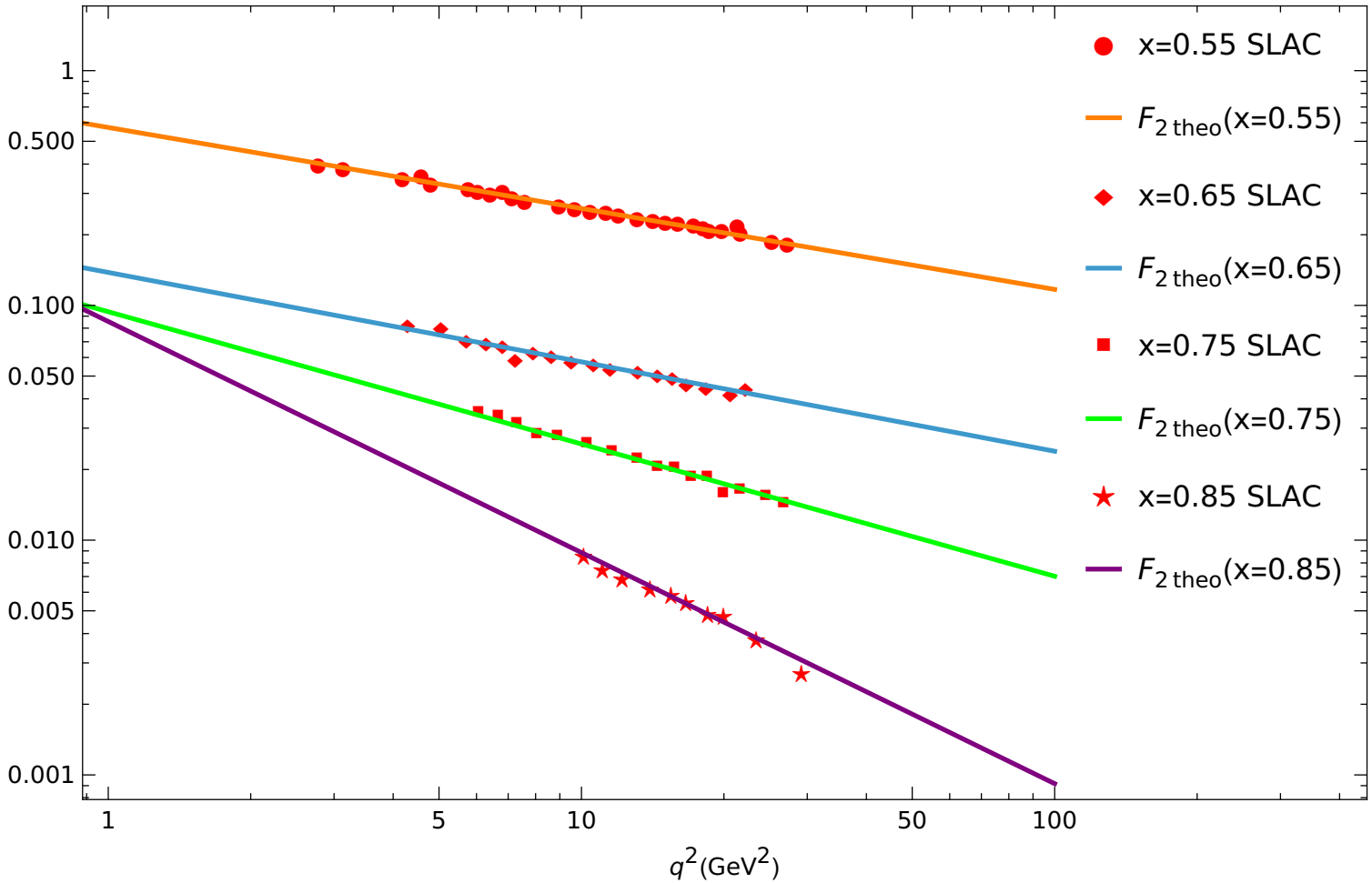

Figura 1: *Proton structure function F_2 as a function of q^2 for fixed values of x. Different points correspond to SLAC data [Whitlow et al., 1992], while the solid lines are our results, Eq. (37), for each value of x.*

Summary of results and Conclusions

Deformed AdS model

- Interesting comparison between its predictions on GFFs of the proton and up to date lattice QCD data, as well as with other holographic results
- Similar results on the mechanical properties of the proton with a dipole approximation compared to lattice and experimental results

Eistein Dilaton model

- Adjustment implemented for a confining schrodinger potential
- Nice fittings of F_2 for large x data
- Need for statistical treatment on the free parameters

Thank you!

Any questions?

References I

Andreev, O. and Zakharov, V. I. (2006).
Heavy-quark potentials and AdS/QCD.
Phys. Rev. D, 74:025023.

Finazzo, S. I. and Noronha, J. (2014).
Debye screening mass near deconfinement from holography.
Phys. Rev. D, 90(11):115028.

Gubser, S. S. and Nellore, A. (2008).
Mimicking the QCD equation of state with a dual black hole.
Phys. Rev. D, 78:086007.

Hackett, D. C., Pefkou, D. A., and Shanahan, P. E. (2024).
Gravitational Form Factors of the Proton from Lattice QCD.
Phys. Rev. Lett., 132(25):251904.

References II

Maldacena, J. M. (1998).
The Large N limit of superconformal field theories and supergravity.
Adv. Theor. Math. Phys., 2:231–252.

Navas, S. et al. (2024).
Review of particle physics.
Phys. Rev. D, 110(3):030001.

Polchinski, J. and Strassler, M. J. (2003).
Deep inelastic scattering and gauge / string duality.
JHEP, 05:012.

Polyakov, M. V. and Schweitzer, P. (2018).
Forces inside hadrons: pressure, surface tension, mechanical radius, and all that.
Int. J. Mod. Phys. A, 33(26):1830025.

References III


Shanahan, P. E. and Detmold, W. (2019).
Gluon gravitational form factors of the nucleon and the pion from lattice QCD.
Phys. Rev. D, 99(1):014511.


Whitlow, L. W., Riordan, E. M., Dasu, S., Rock, S., and Bodek, A. (1992).
Precise measurements of the proton and deuteron structure functions from a global analysis of the SLAC deep inelastic electron scattering cross-sections.
Phys. Lett. B, 282:475–482.